Data-Based Predictive Control for Power Congestion Management in Subtransmission Grids Under Uncertainty

Nouha Dkhili, Sorin Olaru, Alessio Iovine, Guillaume Giraud, Jean Maeght, Patrick Panciatici, Manuel Ruiz

Data-based predictive control for power congestion management in sub-transmission grids under uncertainty

Nouha Dkhili, Sorin Olaru, Alessio Iovine, Guillaume Giraud, Jean Maeght, Patrick Panciatici, Manuel Ruiz

***Abstract*—The energy transition of power grids has spawned a large spectrum of new technical challenges at the design, deployment and operation levels. From a control standpoint, the integration of renewable-energy-based power generation sources into the power grid translates into emerging uncertainties which compromise the system's safety, stability and performance. This paper proposes a model-based predictive controller that incorporates the stochastic nature of these sources into its feedback decision-making policy. The overarching objective is to balance upholding operational constraints of power lines with smart power generation curtailment and energy storage strategies. The proposed method introduces a novel characterization of disturbance trajectory scenarios and their incorporation into the optimisation problem is detailed leading to a robust congestion management strategy. Simulation results are discussed with respect to a baseline of a trend-based disturbance estimation.**

***Index Terms*—Smart grids, congestion management, power systems, model-based predictive control, data-based control, relaxation, convex optimisation, robustness.**

I. Introduction

In order to reconcile ever-growing energy demand with the urgent and paramount need for reducing fossil-fuel-based power generation, power grids require fundamental changes on both physical and cyber fronts. To this end, the deployment of renewable-energy-based power generation sources, also referred to as distributed generation, is a key step towards increasing their efficiency, flexibility and, most importantly, sustainability.

As more and more renewable-energy-based power plants are connected directly to transmission grids, transmission system operators (TSO) are pursuing the digital transformation jointly with the design of new methods for congestion management that can handle the added levels of complexity [1]. It goes without saying that strategies that require minimal infrastructure changes are preferred. As such, flexible asset management is an increasingly popular area of interest in scientific literature [2, 3, 4, 5, 6]. The premise is to use local levers connected to the sub-transmission grid to minimise violations of the powers lines' operational power limits (see [7]). Since renewable power production is the main cause of congestion in modern transmission grids, a powerful option to solve congestion is through renewable power curtailment [8, 9]. Indeed, an overproduction of renewable power directly impacts the transmission lines to operate closer to or beyond their thermal limits [10], and therefore renewable power curtailment is a compelling option to add to classical power congestion strategies [11] and recent ones [12, 13].

In the case study presented in this paper, several renewable power generation plants are connected to a sub-transmission grid. A model-based predictive controller (MPC) determines optimal setpoints for partial curtailment of the plants' generation and for battery usage within the considered zone. Furthermore, aside from the multivariable constrained handling, one of the major difficulties for the controller is to take into account the stochastic nature of the distributed generation in its decision-making [14].

The present paper falls in the research line of using MPC on a modeling of the sub-trasmission grid based on Power Transfer Distribution Factor (PTDF) (see [15, 16]), similarly to the preliminary works in [17] and [18]. The current objective in this research line focuses on the challenges generated by uncertainties due to limited local information and the stochastic nature of renewable power generation. There are several ways to deal with this uncertainty: the safest approach is for the controller to use the worst disturbance trajectory in terms of constraint violation [19]. This approach guarantees robustness but is extremely conservative and significantly restricts the controller's room for maneuver. Also on the conservative side is a trend-based approach as the one considered in [17], where the controller assumes that the disturbance trend observed over the last time step persists over the entire prediction horizon, with simulation results proving that the controller is able to successfully maintain power levels within prescribed margins. There, the authors provide a controllability analysis with respect to the saturation effects of the control inputs acting on the considered time-delayed

Nouha Dkhili, Sorin Olaru and Alessio Iovin are with the Laboratory of Signal and Systems (L2S), Centre National de la Recherche Scientifique (CNRS), CentraleSupélec, Paris-Saclay University, 3, rue Joliot-Curie, 91192 Gif-sur-Yvette, France.
Emails: firstname.lastname@centralesupelec.fr

Guillaume Giraud, Jean Maeght, Patrick Panciatici, Manuel Ruiz are with Réseau de Transport d'Electricité (RTE), Paris, France
Emails: firstname.lastname@rte-france.com

This work was carried out within the CPS4EU project, which has received funding from the ECSEL Joint Undertaking (JU) under grant agreement No 826276. The JU receives support from the European Union's Horizon 2020 research and innovation program and France, Spain, Hungary, Italy, Germany. The proposed results reflect only the authors' view. The JU is not responsible for any use that may be made of the information the present work contains.

model. Moreover, *ad hoc* strategies to ensure practical feasibility and to correctly prioritise the available control action were implemented. Theoretical guarantees were offered for the disturbance realizations that are covered by the trajectories following a constant trend along the prediction horizon. However, the observed robustness comes at the cost of early triggering of power generation curtailment, in particular for this kind of systems that present actuation delays (see [20]). This is a significant drawback since it reduces the strategy's economic attractiveness and goes against the intention of maximising renewable energy penetration in the grid. As a result, a less conservative path must be investigated to integrate renewable intermittence into the controller's decision-making.

There exists a plethora of control applications where the system's behaviour is influenced by one or several disturbances of stochastic nature. The well-established theory of stochastic control tackles these kinds of problems [21]. Stochastic methods offer a richer description of disturbance behaviour to the controller, at the cost of increase in computational and memory requirements. In a MPC framework, dealing with stochastic disturbances in convex optimization problems is quite often done through scenario-based approaches [22]: they provide probabilistic guarantees that the solution of the sample problem satisfies the original chance constrained problem [23]. The literature is rife with examples of sampling-based methods [24, 25, 26, 27, 28], popular thanks to their computationally tractable nature. However, usually these approaches consider reach enough scenarios (and computational times) [26] and predict the mean expectations of the performances [25, 27]. Often, the stochasticity is dealt offline [25]. On the contrary, in the present paper we focus on online short-term optimisation problems, that requires solutions to be computed in few seconds by concentrating on the scenarios characterised by low-probablity but high-impact with respect to the constraints. For this reason, we do not exploit the full range of probabilistic trajectories, but rather focus on few of them according to application-driven selection criteria.

In a similar vein of aforementioned sampling-based approaches, the strategy proposed in this paper follows a sampling-based predictive control approach. First, the uncertain disturbance trajectories need to be generated over a finite horizon. Then, their weighted combination is incorporated into the optimisation problem of the predictive controller. As opposed to the common custom of random sampling from the set of possible trajectories, herein we extend the preliminary results in [18]. In [18], the novel formulation of the optimisation problem incorporating a weighted combination of probabilistic trajectories is presented. In the present paper, we introduce the methodology of constructing these trajectories based on data-driven probability distribution and an iterative process to generate these trajectories over the prediction horizon. In order to produce a fair comparison with respect to the approach in [17], the same time-delay modeling describing partial power curtailment possibilities and introduced in [20] is preserved here. It extends previous modeling that only allowed on/off decisions on power curtailment (see [29, 30]). For the same reason, we consider also the same benchmark describing a real sub-transmission area in France as case study of interest [20, 1].

The paper is organised as follows: section II details the control-oriented system model. Then, section III describes the case study treated in this paper. Next, section IV introduces the proposed prediction-based control strategy. In section V, the methodology used to generate the disturbance trajectories to be handled by the controller is detailed. Analysis of the simulation results is conducted in section VI. The paper ends with a discussion of future research steps in section VII.

II. Modelling

In this section, the dynamical model considered for describing a sub-transmission area is described, as well as its state-space representation.

A. Notations

Let us consider the following notations throughout the paper:

- $\mathcal{Z}^N$ is the set of nodes in the considered zone n^N being its cardinality. P_n^T is the power generated in the transmission network flowing from the exterior of the zone of interest towards the node $n \in \mathcal{Z}^N$.
- $\mathcal{Z}^C \subset \mathcal{Z}^N$ is the set of nodes where the curtailment of the generated power is allowed, n^C being its cardinality. P_n^G is the generated power, while P_n^C is the curtailed one at node $n \in \mathcal{Z}^C$. P_n^A is the available renewable power that can be generated at each sampling time.
- $\mathcal{Z}^B \subset \mathcal{Z}^N$ is the set of nodes with a storage capacity (battery), n^B being its cardinality. P_n^B is the power injected from the battery on node $n \in \mathcal{Z}^C$, while E_n^B describes the battery energy at the same node.
- $\mathcal{Z}^L \subset \{(i,j) \in \{1,...,n^N\} \times \{1,...,n^N\}\}$ is the set of power lines within the zone, n^L being its cardinality. F_{ij} represents the power flow on the line ij.

The operator *diag* describes a diagonal matrix composed by the considered elements. The operator *col* produces a single column vector composed by the aggregation of other vectors. That is, given m vectors $s_i \in \mathbb{R}^n$, $i = 1, ..., m$, the resulting vector $s = col[s_i], i = 1, 2, \ldots, m$, will be:

$$s = col[s_i] = [\ s_1^\mathcal{T}\ \ s_2^\mathcal{T}\ \ ...\ \ s_m^\mathcal{T}\ ]^\mathcal{T} \in \mathbb{R}^{nm}. \tag{1}$$

B. State representation

The state variables characterizing the energy transmission are: the power flows on the lines F_{ij}, the curtailed power P_n^C, the battery power output P_n^B, the battery energy E_n^B, and the generated power P_n^G. The delayed control inputs are the power variations ΔP_n^B and ΔP_n^C. The disturbance ΔP_n^T is unknown, as it represents the power variations in the nodes outside the operated zone. Finally, the variation ΔP_n^G of the generated power P_n^G is known at time instant k based on the state, control

inputs and context information within the zone (namely the available power P_n^A).

The available power P_n^A at time instant k is communicated to the TSO through a SCADA system, but its variation along the prediction horizon is stochastic, as a result of the intermittent nature of wind power generation. Consequently, the values of ΔP_n^G along the prediction horizon are implicitly defined with respect to forecasts of P_n^A and ΔP_n^A, and to the stored values of P_n^G in relationship with P_n^C.

The dynamical model is formulated in a compact form in (2) with b_{ij}^n constant parameters given by PTDF computations, c_n^B the constant power reduction factors for the batteries, and $d \geq 1$ and $\tau \geq 1$ the operational latency due to the communication-delay for the control actions with respect to the battery power output and power curtailment for the generators, respectively. We consider the batteries to act faster with respect to the possibility to curtail renewable power, and consequently $\tau \geq d$.

$$\begin{cases} F_{ij}(k+1) = & F_{ij}(k) + \underbrace{\sum_{n\in\mathcal{Z}^B} b_{ij}^n \Delta P_n^B(k-d)}_{\text{battery}} \\ & + \underbrace{\sum_{n\in\mathcal{Z}^C} b_{ij}^n \left[\Delta P_n^G(k) - \Delta P_n^C(k-\tau)\right]}_{\text{renewables}} \\ & + \underbrace{\sum_{n\in\mathcal{Z}^N} b_{ij}^n \Delta P_n^T(k)}_{\text{periphery}} \\ P_n^C(k+1) = & P_n^C(k) + \Delta P_n^C(k-\tau),\ \forall\ n \in \mathcal{Z}^C \\ P_n^B(k+1) = & P_n^B(k) + \Delta P_n^B(k-d),\ \forall\ n \in \mathcal{Z}^B \\ E_n^B(k+1) = & E_n^B(k) - Tc_n^B[P_n^B(k) + \Delta P_n^B(k-d)], \\ & \forall\ n \in \mathcal{Z}^B \\ P_n^G(k+1) = & P_n^G(k) + \Delta P_n^G(k) - \Delta P_n^C(k-\tau), \\ & \forall\ n \in \mathcal{Z}^C \end{cases} \tag{2}$$

In particular, the term $\Delta P_n^G(k)$, is defined as

$$\Delta P_n^G(k) = \min\left(f_n^G(k), g_n^G(k)\right), \tag{3}$$

with

$$f_n^G(k) = P_n^A(k) + \Delta P_n^A(k) - P_n^G(k) + \Delta \hat{P}_n^C(k-\tau), \tag{4}$$

$$g_n^G(k) = \overline{P}_n^G - P_n^C(k) - P_n^G(k). \tag{5}$$

where $\overline{P}_n^G > 0$ is the maximum installed generating capacity of the renewable power plants in the sub-transmission grid, with $\forall n \in \mathcal{Z}^C$, and the value of $\Delta \hat{P}_n^C(k)$ is defined in the following. Accordingly, the proposed modeling allows for the possibility to pre-compute the term $\Delta P_n^G(k)$ based on values of $P_n^A(k)$, $P_n^G(k)$, $P_n^C(k)$, $\Delta P_n^A(k)$, and $\Delta P_n^C(k)$, while maintaining the system's linearity with respect to the control signal $\Delta P^C(k)$ via the offline computation of the min(.). A more detailed discussion of this approach is provided in [17].

Consequently, the computational burden of dedicated model-based predictive control laws remains minimal since the convex optimisation structure of the problem is preserved. This is a key factor in making the controller suitable for real-time implementation, the preferred setting in light of the reaction times required by TSOs for congestion management.

To describe the model in a compact form, we define:

$$F = col[F_{ij}],\ \forall\ (i,j) \in \mathcal{Z}^L; \tag{6a}$$

$$P^C = col[P_n^C],\ \Delta P^C = col[\Delta P_n^C],\ \forall\ n \in \mathcal{Z}^C; \tag{6b}$$

$$P^B = col[P_n^B],\ \forall\ n \in \mathcal{Z}^B; \tag{6c}$$

$$E^B = col[E_n^B],\ \Delta P^B = col[\Delta P_n^B],\ \forall\ n \in \mathcal{Z}^B; \tag{6d}$$

$$\Delta P^T = col[\Delta P_n^T],\ \forall\ n \in \mathcal{Z}^N; \tag{6e}$$

$$P^G = col[P_n^G],\ \Delta P^G = col[\overline{P}_n^G],\ \forall\ n \in \mathcal{Z}^C. \tag{6f}$$

Now, let us define

$$x(k) = [F(k)\ \ P^C(k)\ \ P^B(k)\ \ E^B(k)\ P^G(k)]^{\mathcal{T}}, \tag{7}$$

$$u_C(k) = \Delta P^C(k),\ \ u_B(k) = \Delta P^B(k), \tag{8}$$

$$w(k) = \Delta P^G(k),\ \ \zeta(k) = \Delta P^T(k). \tag{9}$$

In order to deal with the known actuator delays $\tau \geq 1$ and $d \geq 1$, we define an extended state $\tilde{x}$ as

$$\tilde{x}(k) = [x(k)\ u_C(k-\tau)\ ...\ u_C(k-1)\ u_B(k-d)\ ...\ u_B(k-1)]^{\mathcal{T}}. \tag{10}$$

The resulting dynamical system is as follows:

$$\tilde{x}(k+1) = \tilde{A}\tilde{x}(k) + \underbrace{\begin{bmatrix} \tilde{B}_C\ \tilde{B}_B \end{bmatrix}}_{\tilde{B}} \underbrace{\begin{bmatrix} u_C(k) \\ u_B(k) \end{bmatrix}}_{u(k)} + \underbrace{\begin{bmatrix} \tilde{D}_w\ \tilde{D}_\zeta \end{bmatrix}}_{\tilde{D}} \underbrace{\begin{bmatrix} w(k) \\ \zeta(k) \end{bmatrix}}_{\eta(k)} \tag{11}$$

Without loss of generality, we show here the matrices in the case $\tau \geq 1$ and $d = 1$:

$$\underbrace{\begin{pmatrix} A & B_C & \mathbb{0} & \dots & \mathbb{0} & B_B & \mathbb{0} \\ \mathbb{0} & \mathbb{0} & \mathbb{1} & \mathbb{0} & \mathbb{0} & \mathbb{0} & \mathbb{0} \\ \vdots & \mathbb{0} & \mathbb{0} & \ddots & \mathbb{0} & \vdots & \vdots \\ \mathbb{0} & \mathbb{0} & \dots & \mathbb{0} & \mathbb{1} & \mathbb{0} & \mathbb{0} \\ \mathbb{0} & \mathbb{0} & \mathbb{0} & \mathbb{0} & \mathbb{0} & \mathbb{0} & \mathbb{0} \\ \mathbb{0} & \mathbb{0} & \mathbb{0} & \mathbb{0} & \mathbb{0} & \mathbb{0} & \mathbb{1} \\ \mathbb{0} & \mathbb{0} & \mathbb{0} & \mathbb{0} & \mathbb{0} & \mathbb{0} & \mathbb{0} \end{pmatrix}}_{\tilde{A}}, \underbrace{\begin{pmatrix} \mathbb{0} \\ \mathbb{0} \\ \vdots \\ \mathbb{0} \\ \mathbb{1} \\ \mathbb{0} \\ \mathbb{0} \end{pmatrix}}_{\tilde{B}_C}, \underbrace{\begin{pmatrix} \mathbb{0} \\ \mathbb{0} \\ \vdots \\ \mathbb{0} \\ \mathbb{0} \\ \mathbb{0} \\ \mathbb{1} \end{pmatrix}}_{\tilde{B}_B}, \tag{12}$$

$$\tilde{D}_w = \begin{pmatrix} D_w & \mathbb{0} & \dots & \mathbb{0} & \mathbb{0} & \mathbb{0} & \mathbb{0} \end{pmatrix}^T, \tag{13}$$

$$\tilde{D}_\zeta = \begin{pmatrix} D_\zeta & \mathbb{0} & \dots & \mathbb{0} & \mathbb{0} & \mathbb{0} & \mathbb{0} \end{pmatrix}^T, \tag{14}$$

where the matrices $\mathbb{1}$ and $\mathbb{0}$ have appropriate dimensions with respect to the state $\tilde{x}$ size, and to the delays τ and d, and

$$A = \begin{pmatrix} \mathbb{1}_{\mathbf{n^L}\times\mathbf{n^L}} & \mathbb{0}_{\mathbf{n^L}\times\mathbf{n^C}} & \mathbb{0}_{\mathbf{n^L}\times\mathbf{n^B}} & \mathbb{0}_{\mathbf{n^L}\times\mathbf{n^B}} & \mathbb{0}_{\mathbf{n^L}\times\mathbf{n^C}} \\ \mathbb{0}_{\mathbf{n^C}\times\mathbf{n^L}} & \mathbb{1}_{\mathbf{n^C}\times\mathbf{n^C}} & \mathbb{0}_{\mathbf{n^C}\times\mathbf{n^B}} & \mathbb{0}_{\mathbf{n^C}\times\mathbf{n^B}} & \mathbb{0}_{\mathbf{n^C}\times\mathbf{n^C}} \\ \mathbb{0}_{\mathbf{n^B}\times\mathbf{n^L}} & \mathbb{0}_{\mathbf{n^B}\times\mathbf{n^C}} & \mathbb{1}_{\mathbf{n^B}\times\mathbf{n^B}} & \mathbb{0}_{\mathbf{n^B}\times\mathbf{n^B}} & \mathbb{0}_{\mathbf{n^B}\times\mathbf{n^C}} \\ \mathbb{0}_{\mathbf{n^B}\times\mathbf{n^L}} & \mathbb{0}_{\mathbf{n^B}\times\mathbf{n^C}} & -A_b & \mathbb{1}_{\mathbf{n^B}\times\mathbf{n^B}} & \mathbb{0}_{\mathbf{n^B}\times\mathbf{n^C}} \\ \mathbb{0}_{\mathbf{n^C}\times\mathbf{n^L}} & \mathbb{0}_{\mathbf{n^C}\times\mathbf{n^C}} & \mathbb{0}_{\mathbf{n^C}\times\mathbf{n^B}} & \mathbb{0}_{\mathbf{n^C}\times\mathbf{n^B}} & \mathbb{1}_{\mathbf{n^C}\times\mathbf{n^C}} \end{pmatrix}, \tag{15}$$

$$B_C = \begin{pmatrix} -M_c \\ \mathbb{1}_{\mathbf{n^C}\times\mathbf{n^C}} \\ \mathbb{0}_{\mathbf{n^B}\times\mathbf{n^C}} \\ \mathbb{0}_{\mathbf{n^B}\times\mathbf{n^C}} \\ -\mathbb{1}_{\mathbf{n^C}\times\mathbf{n^C}} \end{pmatrix}, \quad B_B = \begin{pmatrix} M_b \\ \mathbb{0}_{\mathbf{n^C}\times\mathbf{n^B}} \\ \mathbb{1}_{\mathbf{n^B}\times\mathbf{n^B}} \\ -A_b \\ \mathbb{0}_{\mathbf{n^C}\times\mathbf{n^B}} \end{pmatrix}, \tag{16}$$

$$D_w = \begin{pmatrix} M_c & \mathbb{0}_{\mathbf{n^C}\times\mathbf{n^C}} & \mathbb{0}_{\mathbf{n^B}\times\mathbf{n^C}} & \mathbb{0}_{\mathbf{n^B}\times\mathbf{n^C}} & \mathbb{1}_{\mathbf{n^C}\times\mathbf{n^C}} \end{pmatrix}^T, \tag{17}$$

$$D_\zeta = \begin{pmatrix} M_t & \mathbb{0}_{\mathbf{n^C}\times\mathbf{n^N}} & \mathbb{0}_{\mathbf{n^B}\times\mathbf{n^N}} & \mathbb{0}_{\mathbf{n^B}\times\mathbf{n^N}} & \mathbb{0}_{\mathbf{n^C}\times\mathbf{n^N}} \end{pmatrix}^T, \tag{18}$$

with $A_b = diag[Tc_n^B]$, $\forall\ n \in \mathcal{Z}^B$, and M_c, M_b and M_t that are composed by the elements b_{ij}^n of the PTDF matrix described in (2). The k^{th} line in these matrices corresponds to the PTDF of the k^{th} line of F_{ij} at nodes where generation can be curtailed, at nodes where a battery is installed or at nodes where the injections may vary, respectively. The proposed not-delayed system in (11) is equivalent to the delayed one in (2).

Remark 1: Reactive voltage aspects are not considered in this work. This modeling is adapted to identify in real-time the need for acting on curtailment or storage charge/discharge. Alternate Current (AC) feasibility is a consequence of online updates of $cos(\phi)$ from active power and current real-time measurements, where $cos(\phi)$ is the usual power/current ratio at each bus. Moreover, voltage control aspects are out of the scope of this controller, as the zones considered for congestion problems are different from the ones that are defined from a voltage point of view. The temperature and voltage constraints on the power lines are modeled by the maximum power values to be considered as constraints in the optimisation problem. From the storage point of view, due to the high voltages that we consider, the efficiency with respect to power losses for the power flowing to/from the storage device is negligible.

III. Case study

The case study used in this paper is analogous to the one used in [17]. It is a sub-transmission zone whose topology and connections to the rest of the transmission grid are depicted in Figure 1. In this paper, we consider four wind parks to be connected to nodes 2076, 2745, 4720, and 10000 of maximum power generations 66 MW, 54 MW, 10 MW, and 78 MW, respectively. A battery of power capacity 10 MW is connected to node 10000.

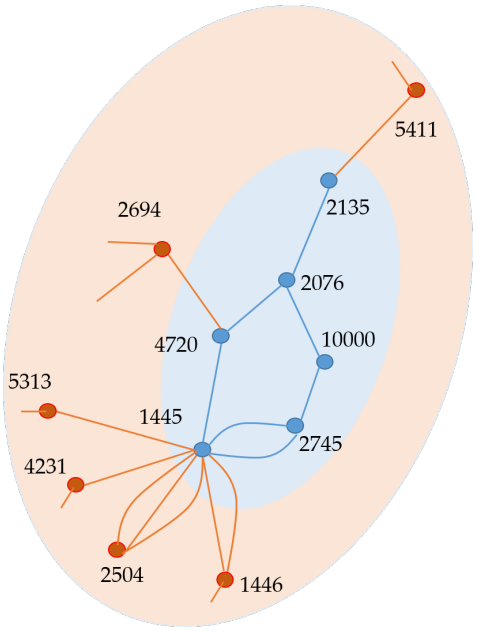

Fig. 1. The considered zone (blue nodes) and its connection to the entire power network (red nodes). The power flow interaction among the blue nodes and the red nodes is described as an uncontrolled generated/absorbed power and thus assimilated as unknown disturbances in the decision-making process.

The wind power generation data used in this study are displayed in Figure 2.

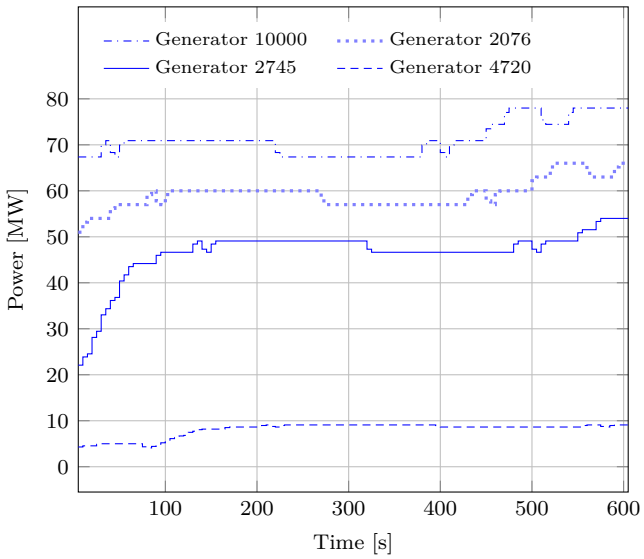

Fig. 2. wind power generation data used in the case study.

The following working hypotheses are considered:

1) each generator produces the maximum available renewable-energy-based power but this will be bounded by the maximum allowed power (this last one is a decision variable, controlled through curtailment actions);

2) only a higher-level controller can decrease the power curtailment setpoints. For this reason, the proposed controller deals only with curtailment increase;
3) the controller does not have access to information regarding the disturbances related to absorbed/generated power elsewhere in the grid (i.e., outside the studied sub-transmission zone). As such these disturbances are considered null;
4) the state of charge (SOC) of the battery is updated each second by a SCADA system. Taking into account the high voltages and the fast dynamics of the batteries, losses within the storage system (conversion, cooling and transformers) will be neglected. A different control level is supposed to manage the SOC with respect to longer time horizons (see [31]);
5) the loads are constant.

IV. MPC integrating uncertainty on the power generation

The control goal is introduced in this section at first. Then, the optimal control problem with respect to the number of considered trajectories and associated probabilities is given.

A. Introduction

The objective of this work is to maintain power flow on the transmission power lines within the regulatory bounds at all times. The chosen strategy is to optimally operate the flexible assets within the zone at a minimal economic cost. In practical terms, the controller uses a storage unit (battery) and partial curtailment of wind power generation[1].

The latter lever incurs economic costs in the form of under-exploitation of the renewable energy infrastructure when the curtailment setpoints issued to the wind parks result in their generation being below the available power levels. Therefore, the controller must walk the line between ensuring operational security and minimizing curtailment of wind power generation.

Moreover, it must take into account the intermittence of renewable-energy-based power generation, which translates into an uncertainty characterisation problem. To address this issue, at each time step, the controller generates possible trajectories for the intermittent power generation (seen as a disturbance from the controller point of view) over the prediction horizon N. Then, it weaves a combination of said trajectories into the optimisation problem. This new formulation allows the controller to select the best control strategy over a finite horizon.

Ideally, the controller should be able to span all the potential trajectories, but this is infeasible in practice due to the completeness of the set $\mathcal{W}$ of disturbance values and the exponential complexity of the number of trajectories with respect to the length of the prediction horizon. Indeed, if $w(k) \in \mathcal{W}$ then the trajectory $[w(k) \dots w(k+N)] \in \mathcal{W}^N$. For this reason, the set $\mathcal{W}$ is sampled so as to have a finite number of possible disturbance values.

The disturbance trajectories and their associated probabilities are considered as input data from the controller's viewpoint. The process driving their selection is detailed in Section V. The discrete values of normalised power generation gradients used to represent their continuous distribution are determined by the method presented in subsection VI-A.

B. Controller design

The proposed control strategy incorporates $N_s > 1$ disturbance trajectories $w(k)$ into the optimisation problem and relaxes the power lines' constraints accordingly. The working assumption is that the N_s scenarios

$$w^j = [w^j(0) w^j(1) \dots w^j(N-1)], \forall j \in \{1, \dots, N_s\}$$

have associated probabilities p^j such that $\sum_1^{N_s} p^j = 1$.

The particular case where $N_s = 1$ is presented in [17]: simulation results have shown that using an extreme disturbance trajectory guarantees robustness but produces very conservative control actions, namely manifesting as preventive curtailment of wind power generation. The objective herein is to better exploit the controller's degrees of freedom while worst case robustness requirements are relaxed all by integrating notions of risk on the constraints satisfaction.

This is reflected in the introduction of a relaxation variable $\varepsilon^j \in \mathbb{R}^N$ such that $j \in \{1, \dots, N_s\}$, which serves to relax the power lines' boundary constraints as follows, $\forall\ i \in [1, N], \quad \forall\ j \in [1, N_s]$:

$$-\overline{L}^j(k+i) \leq F(k+i) \leq \overline{L}^j(k+i) \tag{19}$$

with

$$\overline{L}^j(k+i) = \overline{L} \cdot (1 + \varepsilon^j(k+i)). \tag{20}$$

This relaxation variable reflects a tolerance on the limitations on power flows circulating through the transmission power lines, formulated as a percentage of the regulatory values.

The controller's cost function is therefore defined as:

$$\begin{aligned} J(k) = & \underbrace{\sum_{j=1}^{N_s} p^j \sum_{i=1}^{N} ||\tilde{x}(k+i) - \tilde{x}_r||^2_{\tilde{Q}}}_{\text{reference tracking}} \\ & + \underbrace{\sum_{i=0}^{N} \lambda(i) ||u_C(k+i)||^2_{R_C}}_{\text{curtailment}} + \underbrace{\sum_{i=0}^{N} \theta(i) ||u_B(k+i)||^2_{R_B}}_{\text{battery}} \\ & + \underbrace{\sum_{j=1}^{N_s} \sum_{i=0}^{N} \psi(i,j) p^j \left\| \varepsilon^j(k+i) \right\|^2_{Q_\varepsilon}}_{\text{relaxation}} \end{aligned} \tag{21}$$

where $\tilde{Q}$, R_C, R_B, and Q_ε are square semi-definite positive matrices with respect to the sizes of $\tilde{x}, u_C$, u_B, and ε^j,

[1]The curtailment is partially reversible but this feature is not exploited in the current work which focuses on the uncertainty handling in the prediction model.

respectively. We consider weight functions $\lambda(i)$, $\theta(i)$, and $\psi(i)$. The tuning of weight functions $\lambda(i)$ and $\theta(i)$ strikes the desired balance between action through generation curtailment and battery storage, respectively. For example, a design choice can be to have an increasing function $\theta(i)$ to require faster action of the battery and a decreasing function $\lambda(i)$ that implements a desired behaviour to postpone the curtailment, whenever this is possible. Moreover, to prioritise the utilisation of the battery over the curtailment, it is possible to consider $\lambda(i) > \theta(i)\ \forall i$. The weight function $\psi(i)$ heavily penalises the slack variables ε at prediction step i. Therefore, it ensures that power lines' limits are only relaxed when necessary.

It is worth noticing that disturbance trajectory j is integrated by accounting its probability in both state and relaxation variables.

Now, let us formulate the following set of constraints, $\forall\ i \in [0, N-1]$, $\forall\ j \in [1, N_s]$:

- system dynamics

$$\tilde{x}^j(k+1) = \tilde{A}\tilde{x}^j(k) + \underbrace{\begin{bmatrix} \tilde{B}_C & \tilde{B}_B \end{bmatrix}}_{\tilde{B}} \underbrace{\begin{bmatrix} u_C(k) \\ u_B(k) \end{bmatrix}}_{u(k)} + \underbrace{\begin{bmatrix} \tilde{D}_w^j & \tilde{D}_\zeta \end{bmatrix}}_{\tilde{D}} \underbrace{\begin{bmatrix} w^j(k) \\ \zeta(k) \end{bmatrix}}_{\eta(k)} \tag{22}$$

  These constraints are generated using a pre-determined set of N_s disturbance trajectories. Disturbances originating outside the sub-transmission grid, represented by $\zeta(k)$, are assumed null throughout this paper.

- control input bounds

$$0_{\mathbf{n^C}\times\mathbf{1}} \leq u_C(k+i) \leq \overline{P}^G; \tag{23a}$$

$$\underline{P}^B - \overline{P}^B \leq u_B(k+i) \leq \overline{P}^B - \underline{P}^B. \tag{23b}$$

- extended state bounds

$$\tilde{x}_{\min}(k+i) \leq \tilde{x}(k+i) \leq \tilde{x}_{\max}(k+i), \tag{24}$$

  with

$$\tilde{x}_{\min}(k+i) = [-\overline{L}_i^j\ 0_{\mathbf{n^C}\times\mathbf{1}}\ \underline{P}^B\ \underline{E}^B\ 0_{\mathbf{n^C}\times\mathbf{1}}\ u_{\min}^{\mathcal{T}}]^{\mathcal{T}} \tag{25a}$$

$$\tilde{x}_{\max}(k+i) = [\overline{L}_i^j\ \overline{P}^G\ \overline{P}^B\ \overline{E}^B\ \overline{P}^G\ u_{\max}^{\mathcal{T}}]^{\mathcal{T}} \tag{25b}$$

  where $\overline{L}_i^j$ groups power lines' capacities, $\overline{P}^G > 0$ is the maximum installed generation capacity, $\underline{P}^B < 0$ and $\overline{P}^B > 0$ are bounds of battery power, $\underline{E}^B < 0$ and $\overline{E}^B > 0$ are bounds of battery energy, and $u_{\min}$ and $u_{\max}$ are lower and upper bounds of the control inputs, respectively.

- relaxation parameters' bounds

$$0 \leqslant \varepsilon^j(k+i) \leqslant \varepsilon_{max1} \tag{26}$$

$$\frac{1}{NN_s}\sum_{j=1}^{N_s}\sum_{i=1}^{N}\varepsilon^j(k+i) \leqslant \varepsilon_{max2} \tag{27}$$

  where ε_{max1} is the upper bound of allowed power overshooting on each power line, during each time step, for each trajectory, and ε_{max2} is the upper bound of averaged allowed power overshooting on the power lines, for all considered trajectories.

- weighted relaxation bounds

$$\frac{1}{\tau}\sum_{j=1}^{N_s}\sum_{i=0}^{\tau-1}p^j\varepsilon^j(k+i) \leqslant \varepsilon_{max3} \tag{28}$$

$$\frac{1}{N-\tau}\sum_{j=1}^{N_s}\sum_{i=\tau}^{N}p^j\varepsilon^j(k+i) = 0 \tag{29}$$

  where τ is the curtailment setpoint delay and ε_{max3} is the upper bound of accumulated allowed power overshooting on the power lines, weighted by the trajectories' respective probabilities.
  The relaxation is only allowed in the interval $[k+1, k+\tau]$, to cope with the limitations imposed by the delay on the curtailment action. Once curtailment becomes possible ($[k+\tau+1, N]$), the relaxation is no longer allowed.

Remark 2: The relaxation terms for the hard limitations can be seen as soft constraints in classical predictive control schemes. However, it should be noted that relaxation terms are due to two different reasons. On one hand, due to the delays, a power flow configuration violating the bounds cannot be mitigated instantaneously. Consequently, a relaxation term is needed in order to allow the construction of a control law that brings back the state within the bounds in the shortest time window. This softening of the constraint in this case is linked to the controllability index and cannot be avoided. On the other hand, the fact that several scenarios are considered, allow to weight them accordingly in the constraint handling procedure. The relaxation here is related to the probability distribution and can be tuned through the weights as soon as the corresponding ε is non-zero.

The predictive control problem under uncertainties is defined as:

$$\mathcal{O} = \arg\min_{u_C(k),u_B(k),\ldots,u_C(k+N-1),u_B(k+N-1)} J(k)\ \textit{in}\ (21)$$
$$\textit{subject to constraints}\ ((22)-(29)) \tag{30}$$

The number of possible discrete trajectories of the wind power generation increases exponentially with the length of the prediction horizon. That being said, the proposed approach selects a fixed number of those trajectories to be included in the optimisation problem. As a result, the trajectory generation process becomes computationally heavier as the prediction horizon gets longer but the control problem does not. In fact, the optimisation problem's complexity is linear as a function of the number of trajectories N_s. Indeed, the number of constraints per prediction stage ebing N_c, one has to handle $N_c * N * N_s$ constraints in the current formulation.

Remark 3: Since the goal of this paper is to handle power congestions from the TSO point of view, i.e.,

prioritizing systems safety and reliability over economic aspects, operation costs of storage devices and lifespan are not taken into account, as well as losses in the battery.

V. Probabilistic features of the disturbance trajectories

In this section, we first characterize the experimental construction of a probability of available power variation over time based on the existing recordings. Then, we describe the approach we consider to reduce the needed computational time by considering a pre-defined number of disturbance scenarios in the prediction. It results in an algorithm that implements a heuristic to generate the desired number of trajectories according to a selection strategy that eliminates the least-probable ones but also preserves some realization within the tail of the distribution as they represent a valuable information regarding the risk on the constraint violation.

A. Probability calculations

Let us note c as the number of wind parks with power generation P^{Al} such that $l \in \{1, \dots, c\}$.
Let us note $P^A(k) = [P^{A1}(k) \cdots P^{Ac}(k)]^{\mathcal{T}}$ as the available power generation in the zone at instant k. It follows that the normalised available power generation gradient in the zone is noted $\delta P^A(k) = [\delta P^{A1}(k) \cdots \delta P^{Ac}(k)]^{\mathcal{T}}$, such that $\forall l \in \{1, \dots, c\}$:

$$\delta P^{Al}(k+1) = \frac{P^{Al}(k+1) - P^{Al}(k)}{\overline{\delta P^A}} \tag{31}$$

where $\overline{\delta P^A}$ is the maximum observed variation of P^{Al} over a single time step in the considered database, which gathers wind plant power generation values for a period of one year, sampled at a 5-second rate.

As stated in subsection IV-A, the continuous distribution of gradient values δP^{Al} is represented by discrete ones which can be understood as a classical clustering procedure. Further explanations on the practical test case of the considered application are given in subsection VI-A. Let us note these discrete values as $\delta P^{Al}, \forall l \in \{1, \dots, c\}$.

Thanks to a database containing the power generation of a wind plant over a year, we assume all individual probabilities $\mathbb{P}[\Delta P^{Al}]$ to be known. Then, let us compute:

$$\mathbb{P}[\Delta P^{Al}(k+1) | \Delta P^{Al}(k)].$$

We assume that available power generation of each wind plant is independent from that of the others, i.e.,

$$\mathbb{P}[\Delta P^{Ai}(k) | \Delta P^{Aj}(k)] = \mathbb{P}[\Delta P^{Ai}(k)], \quad \forall i, j \in [1, c]. \tag{32}$$

As a result,

$$\mathbb{P}[\Delta P^A(k)] = \mathbb{P}[\Delta P^{A1}(k) \wedge \cdots \wedge \Delta P^{Ac}(k)] \tag{33}$$

$$= \mathbb{P}[\Delta P^{A1}(k)] * \cdots * \mathbb{P}[\Delta P^{Ac}(k)]. \tag{34}$$

It follows that,

$$\mathbb{P}[\Delta P^A(k) \wedge \Delta P^A(k+1)] = \mathbb{P}[\Delta P^{A1}(k) \wedge \Delta P^{A1}(k+1)] * \cdots * \mathbb{P}[\Delta P^{Ac}(k) \wedge \Delta P^{Ac}(k+1)] \tag{35}$$

Moreover,

$$\mathbb{P}[\Delta P^A(k+1) | \Delta P^A(k)] = \frac{\mathbb{P}[\Delta P^A(k+1) \wedge \Delta P^A(k)]}{\mathbb{P}[\Delta P^A(k)]} \tag{36}$$

and then

$$\mathbb{P}[\Delta P^A(k+1) | \Delta P^A(k)] = \frac{\mathbb{P}[\Delta P^{A1}(k) \wedge \Delta P^{A1}(k+1)] * \cdots * \mathbb{P}[\Delta P^{Ac}(k) \wedge \Delta P^{Ac}(k+1)]}{\mathbb{P}[\Delta P^{A1}(k)] * \cdots * \mathbb{P}[\Delta P^{Ac}(k)]}. \tag{37}$$

The considered zone is equipped with c generators, whose available power generation gradient can take one of μ discrete values. So, there are c^μ possible permutations at each time step. We will denote the set of these alternatives as $\mathcal{M} \subseteq \mathbb{R}^c$.
Furthermore,

$$\sum_{p=1}^{c^\mu} \mathbb{P}[\Delta P^A(k) \wedge \Delta P_p^A(k+1)] = 1 \tag{38}$$

with $\Delta P_p^A(k+1)$ being a given permutation of available power generation gradients in the zone at instant $(k+1)$.

B. Construction of disturbance trajectories

At this point, it is possible to compute probabilities of all possible one-step-ahead trajectories, given information about the present. The combinatorial explosion of the trajectory generation problem poses obvious computational limitations. To resolve this issue, the trajectories are created iteratively. At each step of the forecast horizon, all possible one-step-ahead trajectories are examined and their probabilities computed. Then, a reduced number of trajectories is chosen, denoted N_s. The process then repeats itself as we advance into the forecast horizon.

The clustering procedure used to construct the trajectories of power generation gradient over the forecast horizon is detailed hereinafter.

Let us denote $\Delta P^A(k+t) \in \mathcal{M}, \quad \forall t \in \{1, \dots, N\}$.
We define a given trajectory of available power gradient, $\forall t \in \{1, \dots, N\}$, as:

$$\mathcal{S}^t = \{\Delta P^A(k+1), \dots, \Delta P^A(k+t)\} \in \mathcal{M}^t \tag{39}$$

such that $card(\mathcal{M}^t) = (c^\mu)^t$. The probability of a given trajectory is defined as

$$\mathbb{P}[\mathbb{S}^t(k+1)] = \mathbb{P}[\Delta P_A(k) \wedge \cdots \wedge \Delta P_A(k+t)] \tag{40}$$

The objective is to narrow down the possibilities of the next time step to N_s trajectories, iteratively removing least-probable trajectories. Let us denote the available set of trajectories $\mathcal{R}^t \subseteq \mathcal{M}^t$.
The available set of trajectories is:

- for $t = 1$: $\Delta P^A(k) \in \mathbb{R}^c$ are available as measurements and $\mathcal{R}^1 = \mathcal{M}$.
- for $t \in \{2, \dots, N\}$: $\mathcal{R}^t \subseteq \mathcal{R}^{t-1} \times \mathcal{M}$.

The iterative procedure to trim down the set of possible trajectories starts with the identification of the least-probable trajectory:

$$S^* = \arg\min_{S \in \mathcal{R}^t} \mathbb{P}[S] \tag{41}$$

with

$$p^* = \mathbb{P}[S^*]. \tag{42}$$

Then

$$\mathcal{R}^t = \mathcal{R}^t \setminus \{S^*\} \tag{43}$$

We define the following proximity function:

$$\begin{aligned} \mathcal{N} : \mathcal{S}^t \times \mathcal{S}^t &\longrightarrow \mathbb{R}_+ \\ (S_i, S_j) &\longmapsto \|\mathbb{S}_i - \mathbb{S}_j\|_1 \end{aligned}$$

Then, we identify the closest neighbour to S^* as

$$Q = \min_{S \in \mathcal{R}^t} \mathcal{N}(S^*, S) \tag{44}$$

Once the closest neighbour is identified, it receives the probability of the least-probable trajectory. This translates into

$$\mathbb{P}[Q] = \mathbb{P}[Q] + \mathbb{P}[S^*] \tag{45}$$

The operations described by Equations (41) through (45) are performed:

- $(c^\mu - N_s)$ times in the case $t = 1$.
- $(N_s c^\mu - N_s)$ times for each $t \in \{1, \ldots, N\}$.

Consequently, the cost of the trajectory generation process as a whole grows linearly with respect to the number of selected trajectories N_s.

By the end of this process, we obtain the set of trajectories $\mathcal{R}^N \subseteq \mathcal{M}^N$ such that

$$card(\mathcal{R}^N) = N_s \tag{46}$$

$$card(\mathcal{M}^N) = (c^\mu)^N \tag{47}$$

$$\sum_{S \in \mathcal{R}^N} \mathbb{P}(S) = 1 \tag{48}$$

Let us denote $p^j, \forall j \in \{1, \ldots, N_s\}$ as the probability corresponding to trajectory j.

VI. Numerical results and analysis

This section is broken down into three parts: the first presents the method used to pre-process wind power generation data in order to determine discrete values to represent an otherwise continuous distribution. Then, focus is put on the evaluation of the generated disturbance trajectories. The third part of this section examines the performance of the proposed controller with respect to a conservative reference strategy in terms of inner-zone disturbances.

The power lines' maximum capacities are $\pm 45\,\mathrm{MW}$. Chosen values for the relaxation parameters introduced in section IV are the following: $\varepsilon_{max1} = 0.05$, $\varepsilon_{max2} = 0.2$, $\varepsilon_{max3} = 0.2$.

Simulations presented in this paper are obtained in Matlab2021 over a 10-minute period and considering a time step of 5 s and a prediction horizon $N = 10$, i.e., 50 seconds. The prediction horizon is chosen to be large enough to take into account the largest actuation delay, i.e., $45s$ (9 sampling times), but not too large as this will have a negative impact on the propagation of the prediction errors. To emulate a real power transmission network, the function *runpf* of MATPOWER is used to simulate the AC power flow on the whole transmission network of the French electricity grid [32], [33]. The computer used to run the simulations is an Intel(R) Core(TM) i9-10885H CPU@2.40GHz, with a 32 GB RAM.

A. Pre-processing

$\pm 45\,\mathrm{m}^3$

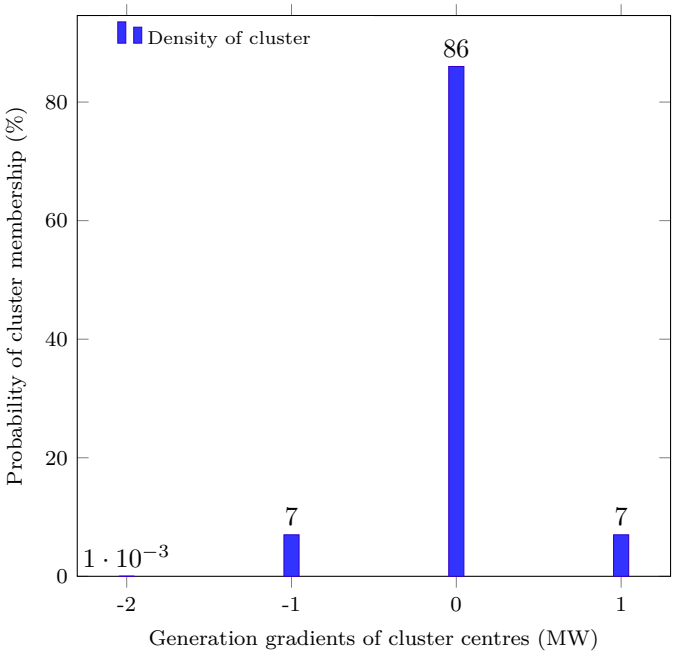

Fig. 3. Obtained clusters of wind power generation gradients in MW.

In order to generate a finite number of possible trajectories over the prediction horizon, we need to consider a finite number μ of discrete values of normalised distributed generation gradients. We choose these values so as to adequately represent the distribution of wind power generation levels in the database.

In order to do so, we perform a clustering process of available values of δP^{Al} into μ clusters using a k-means algorithm implemented in Matlab2021 ([34]). The present approach is independent of this clusterring procedure, any commercially-available clustering algorithms could be used; K-means is chosen here because it is simple, fast, and effective enough for the purposes of this study.

The clustering function can be defined as follows:

$$\begin{aligned} \mathcal{C} : [-1, 1] &\longrightarrow V \\ \delta P^{Al} &\longmapsto \Delta P^{Al} \end{aligned}$$

where $\Delta P^{Al} \in V$ designates the cluster center, and V is the set of clusters' centers such that $card(V) = \mu$. In the rest of the paper, all members of a given cluster are represented by its centre.

Figure 3 displays the distribution of normalised gradient values from the database between the clusters. The cluster centered at zero emerges as significantly larger than the rest, containing 86% of the database, as opposed to 0.001%,

7%, and 7% for the clusters centered at −2 MW, −1 MW, and 1 MW, respectively. It is also worth noting that in the case of this larger cluster, all its members are perfectly identical to its center, i.e., their values are equal to zero. In other words, in this case study, the probability of the wind power generation gradient being zero is 86%. This high probability is a drawback of the small sampling time (5 s).

B. Evaluation of the disturbance trajectories

The disturbance trajectories generated through the process detailed in section V are integrated into the optimisation problem of the predictive controller. The controller's purpose is real-time congestion management in power sub-transmission grids with high levels of renewable-energy-based power generation, namely wind power generation.

Therefore, the main purpose of judicious selection of disturbance trajectories is to enable the controller to minimise overshooting on the power lines of the sub-transmission grid. Consequently, the maximum overshooting observed on the lines is by far the most crucial criterion for evaluating the choice of trajectories. This aspect is thoroughly examined in subsection VI-C.

That being said, the quality of generated disturbance trajectories, with respect to their number, can also be evaluated using the following criteria:

1) impact on the controller's computational cost:
   when replacing a single prediction of the disturbance trajectory with multiple ones, an unmistakable consequence is the added computational cost on the control scheme. Herein, we measure the time needed to simulate 10 minutes of the predictive controller's operation (with a 5-second time step).
2) coverage of a subset of possible trajectories:
   a trajectory $\mathcal{S}_D^N$ 'covers' the subset of trajectories $\mathcal{M}_d^N$, such that $\mathcal{M}_d^N \subseteq \mathcal{M}^N$, if and only if $\mathcal{S}_D^N$ dominates every trajectory $\mathcal{S}_d^N \in \mathcal{M}_d^N$ at each time step, i.e. if and only if

$$\Delta P_D^A(k+t) \geqslant \Delta P_d^A(k+t), \quad \forall t \in \{1, \dots, N\} \quad (49)$$

   where

$$\mathcal{S}_D^N = \{\Delta P_D^A(k+1), \dots, \Delta P_D^A(k+N)\} \quad (50)$$

$$\mathcal{S}_d^N = \{\Delta P_d^A(k+1), \dots, \Delta P_d^A(k+N)\} \quad (51)$$

Figure 4 displays the total time required to simulate 10 minutes of operation of the grid described in section III, with respect to the number of disturbance trajectories N_s that the predictive controller takes into account. The increasing number of trajectories reliably increases the controller's computational cost. Beyond 4 disturbance trajectories, the time required to simulate a period of 10 minutes surpasses that length. One could argue that computational cost can be decreased by code optimisation and use of a faster computer. However, the pattern proves an exponential increase in computational time and clearly represents the main practical restriction. It makes the case for using a small number of carefully-chosen trajectories for this application, over the customary use of a large number of them in classical scenario-based approaches.

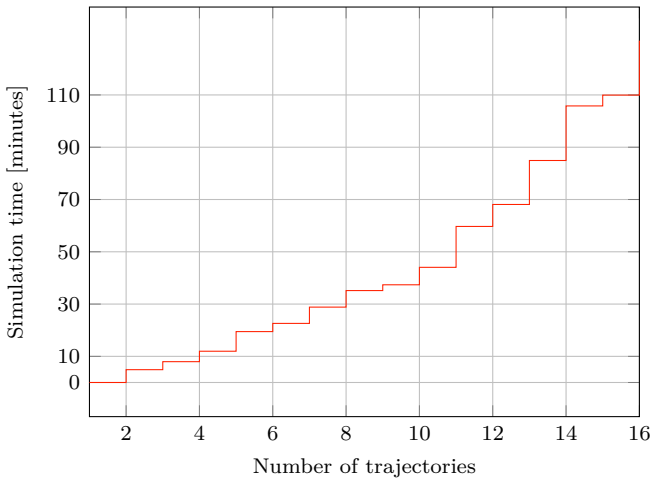

Fig. 4. Total time required to simulate 10 minutes of power grid operation, with respect to the number of selected disturbance trajectories N_s used by the predictive controller.

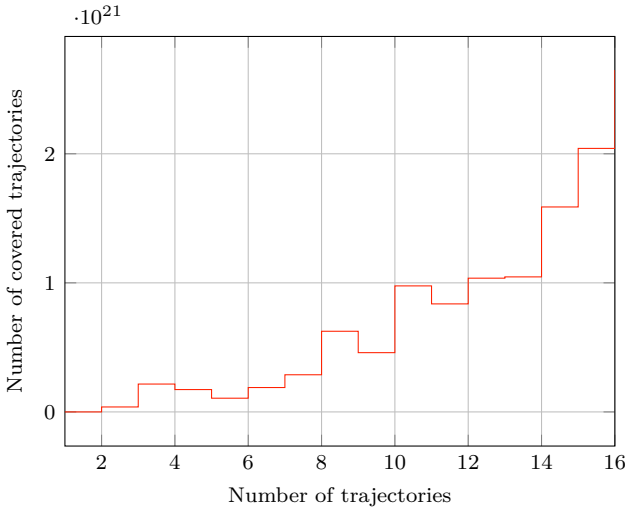

Fig. 5. Number of possible disturbance trajectories covered by the ones selected for the predictive controller, with respect to their number N_s.

Figure 5 displays the number of possible disturbance trajectories that the ones selected for the predictive controller cover, as their number increases. Unsurprisingly, the coverage tends to increase as the number of selected trajectories does, albeit not in a straightforwardly linear pattern as does the number of operations in the selection process.

As a matter of fact, when increasing the number of chosen trajectories, several of them end up being branches of a common probable trunk in the probability tree. The inclusion of these branches in the controller's optimisation problem enable consideration of finer fluctuations in the disturbance's behaviour. However, these neighbour trajectories actually cover very similar subsets of the set of

possibilities according to the definition given by Equation (49). On account of this overlap, additional disturbance trajectories do not necessarily lead to further coverage of the total possibility set.

It should be noted that the percentage of covered trajectories remains small (less than 1% of the set of possibilities) for the cases displayed herein. This is an inherent drawback of the reliance on probability of occurrence as a criterion of selection. In order to mitigate this effect, several techniques can be investigated. For instance, the worst-case trajectory can be manually preserved during the trajectory generation process to account for the extreme case. The drawback of this solution is that it brings us back to the conservative control case. Another option is to introduce a random trajectory into the mix at regular intervals of the selection process in order to favour the exploration of less probable paths, a technique inspired by mutations in genetic algorithms [35].

In the absence of accurate forecasts of wind power generation gradients at such small scales (5-second prediction horizon), the controller relies on the information given by a few carefully-chosen trajectories. In light of both criteria discussed hereinabove, a choice was made to run the predictive controller using 4 disturbance trajectories.

C. Evaluation of the controller's performance

Per the conservative reference strategy, the wind power generation gradient is assumed constant all along the prediction horizon:

$$\Delta P^A(k+i) = \Delta P^A(k), \forall\ i \in [1, N] \tag{52}$$

which leads to

$$P^A(k+N) = P^A(k) + N * \Delta P^A(k). \tag{53}$$

This assumption leads to a conservative generation curve over the prediction horizon, which is more likely to trigger the power lines' boundary constraints more often.

Although such a trajectory is a low-probability one, it is in line with the TSO's strategy of prioritizing safety and operational security. The most obvious drawback from the TSO's viewpoint is that the overestimation of the constraint violation will lead to more aggressive curtailment strategy. Furthermore, this goes against the TSO's objectives since it undermines the promotion of renewable energy and incurs an economic cost.

The proposed sampling-based MPC described in section IV aims to mitigate the economic cost of the conservative strategy by allowing for contained overshooting on the power lines and considering less drastic disturbance trajectories.

In Figure 6, setpoints of the battery power gradient are displayed for both strategies, resulting in the battery power input shown in Figure 7. Figure 8 depicts the wind power generation curtailment profiles for all four wind park generators connected to the sub-transmission grid, while Table I provides the total amount of potential request of power curtailment in MW and compare them in percentage.

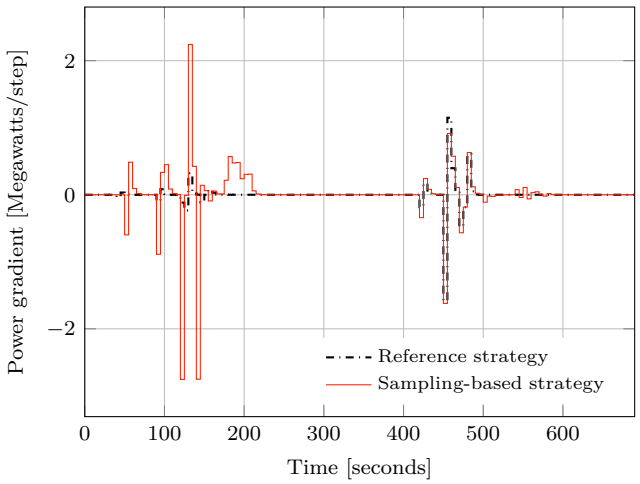

Fig. 6. Gradient of battery power setpoint ΔP_b.

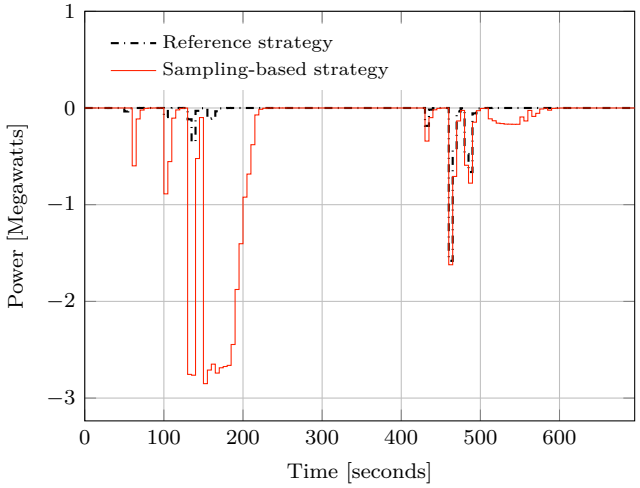

Fig. 7. Battery power input P_b.

The comparison shows a similar trend of gaining around 11% with the sampling-based strategy with respect to the trend-based one in the case of interest. Figure 9 displays the extrema of power flows on the power lines of the sub-transmission grid with respect to their capacities.

Strategy/Node	**10000**	**2076**	**2745**	**4720**
Trend-based [MW]	657.3	473.8	841	122.2
Sampling-based [MW]	584.1	420.7	747.4	108
Comparison [%]	-11.1	-11.2	-11.1	-11.6

TABLE I
THE CURTAILMENT DEMAND IN THE TWO STRATEGIES IN FIG. 8.

As expected, the reference strategy is more conservative: it acts quicker and more aggressively, and on both levers despite the prioritisation of the curtailment in the objective function, in order to prevent overshooting on the power lines before it appears. Nevertheless, this aggressive course of action goes against the control strategy's interest in two

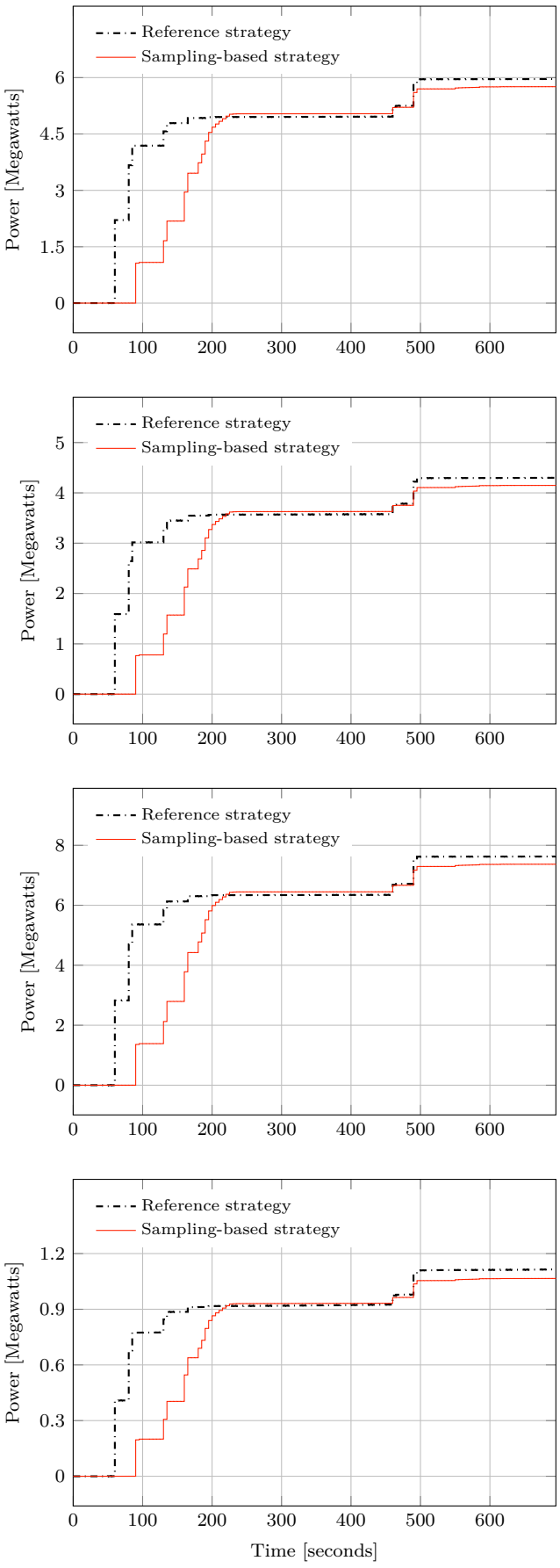

Fig. 8. Curtailed wind power generation P_c for the four generation parks within the sub-transmission grid in the nodes 10000, 2076, 2745 and 4720, respectively. .

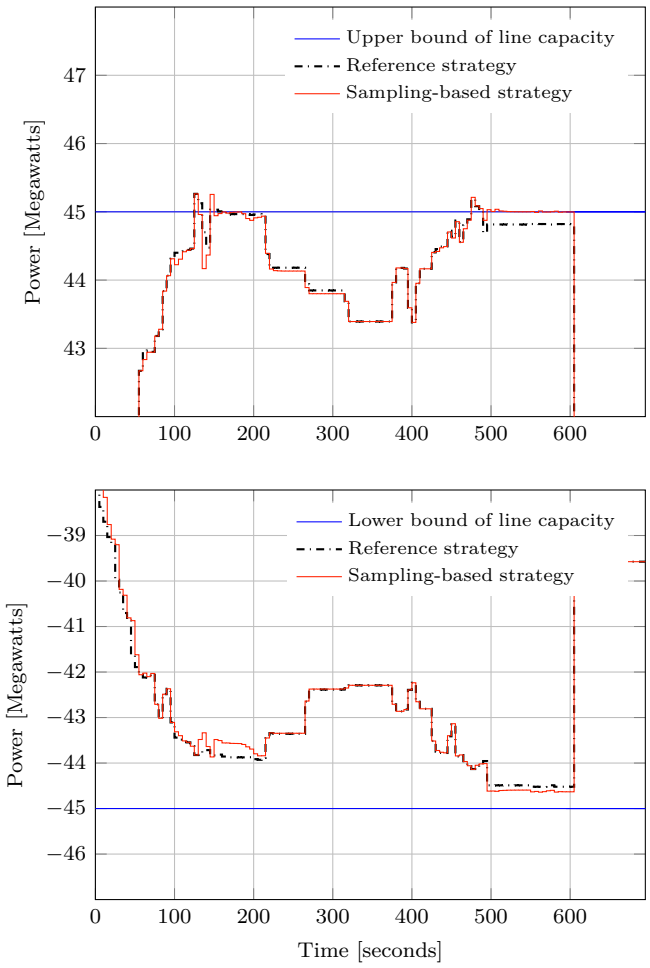

Fig. 9. Extrema of power flows with respect to powers' lines capacities.

main ways. First, it incurs irreversible economic costs as wind power generation is curtailed and cannot be dialled back up without supervisory level intervention. Second, it contradicts with the broader directive of fostering the deployment of renewable-energy-based power generation in power grids. The sampling-based strategy moves in to mitigate these troublesome effects. As it stands, it only intervenes once the constraints are violated, but only within the limits of what the relaxation parameters allow. This is observed first from the beginning of the second minute and then again during the eighth minute of the simulation. As a consequence, it draws more on the battery, with respect to the reference strategy, to reign in the imminent overshooting. The delayed intervention of the sampling-based controller is advantageous since it results in a decrease in curtailment levels for distributed generation with respect to those given by the conservative controller at reasonable constraint violation costs, for the considered case study.

It should be noted that the overshooting on the power lines is only allowed by the sampling-based controller within the limits of the relaxation formulated through Equations (26), (27), and (29). Consequently, the sampling-based controller leans on the contained overshooting on the power

lines to optimise the operation's economic cost without comprising the system's safety.

The introduction of relaxation variables, as explained in subsection IV-B, is justified by the fact that small and brief overshooting over the conservative bounds $(\underline{L}, \overline{L})$ can be handled by the power lines without permanent damage. As a matter of fact, the extension of these bounds to dynamic ones that determine the amplitude and duration of 'safe overshooting' is explored thoroughly in [36]. As a result, values of relaxation bounds ε_{max1}, ε_{max2}, and ε_{max3} are chosen to ensure that the permitted constraint violation remains safe from an operational viewpoint.

The appraisal of the control strategy's performance boils down to a trade-off between minimization of constraint violation (namely of power lines' boundaries) and minimization of wind power generation curtailment and, by extension, optimisation of the economic cost of the wind parks' operation. At the implementation stage, the complexity of the control strategy also comes into play, namely the computational cost of the trajectory generation process. In other terms, the application for which the controller is developed dictates its priorities: the conservative trend-based strategy is better-suited for applications with high security imperatives, while the sampling based method presented herein is shown to give more room for maneuver, at reasonable computational cost, provided some liberty can be taken with constraint violations.

It should be noted that the discussion of the controller actions' economic cost conducted above is focused on the lost revenue of curtailing wind power generation i.e. situations where the wind parks' generated power is less than the available power.

The discussion in this paper disregards the losses due to equipment wear, namely effects of the battery's life span. This is especially the case in the setting where battery use is prioritised over the curtailment. In addition, when it comes the optimisation of battery use, pivotal decisions are the optimal sizing and placement of the batteries in a given sub-transmission grid. There is extensive work in the literature around this focal point [37, 38, 39].

As it stands, as sole battery of power capacity 10 MW is installed in the studied sub-transmission grid, connected to the same node as the wind park of maximum power generation 78 MW (see section III). This placement choice limits is an inherit constraint to the battery's regulatory action. Alternate solutions could be investigated: the sole battery's placement could be optimised within the grid or it could be replaced with several smaller-capacity batteries placed at different nodes.

VII. Conclusion

In this paper, a sampling-based predictive controller is developed for congestion management in sub-transmission grids and its performance is evaluated with respect to a trend-based strategy. A methodology of disturbance trajectory generation is proposed. The integration of these trajectories into the predictive controller's optimisation problem leads to a decrease in wind power generation curtailment when compared to the trend-based method used in [17]. The proposed strategy therefore demonstrates promising economic gains.

Prospects of this work concerns both theoretical aspects and the application-oriented improvements. At first, we target to quantify the error introduced by the considered heuristic with respect to the optimal case with the whole set of scenarios. This will also help in better defining the link with Montecarlo methods, allowing for an analysis of the risk incurred by the selection of a reduced number of disturbance trajectories. Moreover, improvements target optimal sizing and placement of the battery, and study of the economic cost of battery utilisation. At an ulterior step, the handling of uncertainty due to intermittent power generation outside the considered sub-transmission grid remains to be investigated. A similar approach with the one presented here can cope with this source of uncertainty as long as a pertinent family of scenarios can be obtained.

References

[1] B. Meyer, J. Astic, P. Meyer, F. Sardou, C. Poumarede, N. Couturier, M. Fontaine, C. Lemaitre, J. Maeght, and C. Straub, "Power Transmission Technologies and Solutions: The Latest Advances at RTE, the French Transmission System Operator," IEEE Power and Energy Magazine, vol. 18, no. 2, pp. 43–52, 2020.

[2] H. Sugihara, K. Yokoyama, O. Saeki, K. Tsuji, and T. Funaki, "Economic and efficient voltage management using customer-owned energy storage systems in a distribution network with high penetration of photovoltaic systems," IEEE Transactions on Power Systems, vol. 28, no. 1, pp. 102–111, 2012.

[3] I. Prodan and E. Zio, "A model predictive control framework for reliable microgrid energy management," International Journal of Electrical Power & Energy Systems, vol. 61, pp. 399–409, 2014.

[4] C. S. Ioakimidis, D. Thomas, P. Rycerski, and K. N. Genikomsakis, "Peak shaving and valley filling of power consumption profile in non-residential buildings using an electric vehicle parking lot," Energy, vol. 148, pp. 148–158, 2018.

[5] M. Bahramipanah, D. Torregrossa, R. Cherkaoui, and M. Paolone, "A decentralized adaptive model-based real-time control for active distribution networks using battery energy storage systems," IEEE Transactions on Smart Grid, vol. 9, no. 4, pp. 3406–3418, 2018.

[6] U. R. Nair, M. Sandelic, A. Sangwongwanich, T. Dragičević, R. Costa-Castelló, and F. Blaabjerg, "Grid congestion mitigation and battery degradation minimisation using model predictive control in pv-based microgrid," IEEE Transactions on Energy Conversion, vol. 36, no. 2, pp. 1500–1509, 2021.

[7] N. Henka, Q. Francois, S. Tazi, M. Ruiz, and P. Panciatici, "Power grid segmentation for local topological controllers," Electric Power Systems Research, vol. 213, p. 108302, 2022.

[8] I. Liere-Netheler, F. Schuldt, K. von Maydell, and C. Agert, "Optimised curtailment of distributed

generators for the provision of congestion management services considering discrete controllability," IET Generation, Transmission Distribution, vol. 14, pp. 735–744(9), March 2020.

[9] L. Orrù, G. Lisciandrello, G. Coletta, M. De Ieso, S. Gliozzi, M. Ramacciani, and T. D'Aversa, "A short-term congestion management algorithm for the italian subtransmission grid: experimental validation of the osmose zonal-ems," in 2022 AEIT International Annual Conference (AEIT), 2022, pp. 1–6.

[10] G. Coletta, A. Laso, G. M. Jónsdóttir, M. Manana, D. Villacci, A. Vaccaro, and F. Milano, "On-line control of ders to enhance the dynamic thermal rating of transmission lines," IEEE Transactions on Sustainable Energy, vol. 11, no. 4, pp. 2836–2844, 2020.

[11] A. Pillay, S. Prabhakar Karthikeyan, and D. Kothari, "Congestion management in power systems – a review," International Journal of Electrical Power Energy Systems, vol. 70, pp. 83–90, 2015.

[12] Y. Chen, R. Moreno, G. Strbac, and D. Alvarado, "Coordination strategies for securing ac/dc flexible transmission networks with renewables," IEEE Transactions on Power Systems, vol. 33, no. 6, pp. 6309–6320, 2018.

[13] L. Ortmann, C. Rubin, A. Scozzafava, J. Lehmann, S. Bolognani, and F. Dörfler, "Deployment of an online feedback optimization controller for reactive power flow optimization in a distribution grid," 2023.

[14] B. Park, Z. Zhou, A. Botterud, and P. Thimmapuram, "Probabilistic zonal reserve requirements for improved energy management and deliverability with wind power uncertainty," IEEE Transactions on Power Systems, vol. 35, no. 6, pp. 4324–4334, 2020.

[15] A. J. Wood, B. F. Wollenberg, and G. B. Sheblé, Power Generation, Operation, and Control, 3rd Edition. Wiley, 2013.

[16] Xu Cheng and T. J. Overbye, "PTDF-based power system equivalents," IEEE Transactions on Power Systems, vol. 20, no. 4, pp. 1868–1876, 2005.

[17] D.-T. Hoang, S. Olaru, A. Iovine, J. Maeght, P. Panciatici, and M. Ruiz, "Power congestion management of a sub-transmission area power network using partial renewable power curtailment via mpc," Control and Decision Conference. Dec 2021. Austin. Texas. United States, 2021.

[18] N. Dkhili, S. Olaru, A. Iovine, M. Ruiz, J. Maeght, and P. Panciatici, "Predictive control based on stochastic disturbance trajectories for congestion management in sub-transmission grids," IFAC-PapersOnLine, vol. 55, no. 16, pp. 302–307, 2022, 18th IFAC Workshop on Control Applications of Optimization CAO 2022.

[19] J. H. Lee and Z. Yu, "Worst-case formulations of model predictive control for systems with bounded parameters," Automatica, vol. 33, no. 5, pp. 763–781, 1997.

[20] A. Iovine, D.-T. Hoang, S. Olaru, J. Maeght, P. Panciatici, and M. Ruiz, "Modeling the partial renewable power curtailment for transmission network management," 2021 IEEE Madrid PowerTech, pp. 1–6, 2021.

[21] K. J. Åström, Introduction to stochastic control theory. Courier Corporation, 2012.

[22] M. C. Campi and S. Garatti, "A sampling-and-discarding approach to chance-constrained optimization: feasibility and optimality," Journal of optimization theory and applications, vol. 148, no. 2, pp. 257–280, 2011.

[23] T. Alamo, R. Tempo, and E. F. Camacho, "Randomized strategies for probabilistic solutions of uncertain feasibility and optimization problems," IEEE Transactions on Automatic Control, vol. 54, no. 11, pp. 2545–2559, 2009.

[24] M. Korda, R. Gondhalekar, F. Oldewurtel, and C. N. Jones, "Stochastic mpc framework for controlling the average constraint violation," IEEE Transactions on Automatic Control, vol. 59, no. 7, pp. 1706–1721, 2014.

[25] M. Lorenzen, F. Dabbene, R. Tempo, and F. Allgöwer, "Stochastic mpc with offline uncertainty sampling," Automatica, vol. 81, pp. 176–183, 2017.

[26] D. Fioriti and D. Poli, "A novel stochastic method to dispatch microgrids using Monte Carlo scenarios," Electric Power Systems Research, vol. 175, p. 105896, 2019.

[27] M. Prandini, S. Garatti, and J. Lygeros, "A randomized approach to stochastic model predictive control," in 2012 IEEE 51st IEEE Conference on Decision and Control (CDC), 2012, pp. 7315–7320.

[28] J. Paulson, T. Santos, and A. Mesbah, "Mixed stochastic-deterministic tube mpc for offset-free tracking in the presence of plant-model mismatch," Journal of Process Control, vol. 83, pp. 102–120, 2019.

[29] C. Straub, S. Olaru, J. Maeght, and P. Panciatici, "Robust MPC for temperature management on electrical transmission lines," IFAC-PapersOnLine, vol. 51, no. 32, pp. 355 – 360, 2018, 17th IFAC Workshop on Control Applications of Optimization CAO 2018.

[30] ——, "Zonal congestion management mixing large battery storage systems and generation curtailment," IEEE Conference on Control Technology and Applications (CCTA), pp. 988–995, 2018.

[31] C. Straub, J. Maeght, C. Pache, P. Panciatici, and R. Rajagopal, "Congestion management within a multi-service scheduling coordination scheme for large battery storage systems," in 2019 IEEE Milan PowerTech, 2019, pp. 1–6.

[32] R. D. Zimmerman, C. E. Murillo-Sánchez, and R. J. Thomas, "Matpower: Steady-state operations, planning, and analysis tools for power systems research and education," IEEE Transactions on Power Systems, vol. 26, no. 1, pp. 12–19, 2011.

[33] C. Josz, S. Fliscounakis, J. Maeght, and P. Panciatici, "AC Power Flow Data in MATPOWER and QCQP Format: iTesla, RTE Snapshots, and PEGASE," arXiv, 1603.01533, 2016.

[34] A. Kapoor and A. Singhal, "A comparative study

of k-means, k-means++ and fuzzy c-means clustering algorithms," in 2017 3rd international conference on computational intelligence & communication technology (CICT). IEEE, 2017, pp. 1–6.

[35] D. Whitley, "A genetic algorithm tutorial," Statistics and computing, vol. 4, no. 2, pp. 65–85, 1994.

[36] T.-H. Pham, A. Iovine, S. Olaru, J. Maeght, P. Panciatici, and M. Ruiz, "Advanced management of network overload in areas with Renewable Energies Sources," vol. 55, no. 9, 2022, pp. 81–86, 11th IFAC Symposium on Control of Power and Energy Systems CPES 2022.

[37] M. R. Jannesar, A. Sedighi, M. Savaghebi, and J. M. Guerrero, "Optimal placement, sizing, and daily charge/discharge of battery energy storage in low voltage distribution network with high photovoltaic penetration," Applied energy, vol. 226, pp. 957–966, 2018.

[38] K. Khalid Mehmood, S. U. Khan, S.-J. Lee, Z. M. Haider, M. K. Rafique, and C.-H. Kim, "Optimal sizing and allocation of battery energy storage systems with wind and solar power dgs in a distribution network for voltage regulation considering the lifespan of batteries," IET Renewable Power Generation, vol. 11, no. 10, pp. 1305–1315, 2017.

[39] H. Nazaripouya, Y. Wang, P. Chu, H. R. Pota, and R. Gadh, "Optimal sizing and placement of battery energy storage in distribution system based on solar size for voltage regulation," in 2015 IEEE Power & Energy Society General Meeting. IEEE, 2015, pp. 1–5.